Solids Modeled by ab Initio Crystal-Field Methods. 12. Structure, Orientation, and Position of A-Type Carbonate in a Hydroxyapatite Lattice

Anik Peeters,[†] Erna A. P. De Maeyer,[‡] Christian Van Alsenoy,*[,†] and Ronald M. H. Verbeeck[‡]

Chemistry Department, University of Antwerp (UIA), Universiteitsplein 1, B-2610 Wilrijk, Belgium, and Department of Dental Materials Science, University Hospital, University of Ghent, De Pintelaan 185, B-9000 Ghent, Belgium

Received: December 10, 1996; In Final Form: February 26, 1997[⊗]

Using ab initio methods, the position and the orientation of a CO_3^{2-} impurity in a hydroxyapatite lattice is studied. The CO_3^{2-} ion is oriented in a plane that makes an angle of 7° with the crystallographic *c* axis. The carbon atom and two oxygen atoms occupy positions close to the axis, whereas the third oxygen is oriented almost perpendicular to the symmetry axis. For the optimized structure, the vibrational characteristics are in reasonable agreement with the experimental data. The influence of experimentally observed variations of the lattice parameters on the geometry of the CO_3^{2-} impurity is negligible. A study of the potential energy surface indicates that the six symmetry-related equilibrium positions are connected by rotation about the crystallographic *c* axis.

Introduction

$Ca_{10}(PO_4)_6(OH)_2$ (calcium hydroxyapatite, further referred to as HAp) is generally accepted to be the prototype for the mineral phase of the calcified tissues of higher vertebrates such as bone and teeth.[1] Impurities, especially CO_3^{2-}, are known to enhance the susceptibility of these tissues to demineralization, e.g., caries. Carbonate can substitute either for PO_4^{3-} or for OH^- in the apatite lattice, which is called B- and A-type CO_3^{2-}, respectively. This study considers the A-type CO_3^{2-} substitution, which represents 5−10% of the total amount of CO_3^{2-} present in tooth enamel.[2,3]

In the past, some indications were found about the orientation of the A-type CO_3^{2-} ion with respect to the crystallographic *c* axis using structure refinement methods based on X-ray and neutron powder diffraction patterns,[4] polarized IR measurements,[2] and electron spin resonance spectroscopy.[5] Young and co-workers[4] even calculated the positions of the carbon and oxygen atoms. However, because more than one model fit the experimental data equally well, there is a need for additional studies. Moreover, to our knowledge, ab initio calculations were never performed on this system.

In this study, the internal geometry, the position, and the orientation of an A-type CO_3^{2-} impurity in a HAp cavity is optimized quantum mechanically. For the optimized structure of the A-type CO_3^{2-}, vibrational absorptions are calculated and compared with experimental results. Moreover, the influence of a variation of the lattice parameters on the geometry of the CO_3^{2-} ion, the charges on the atoms, and the potential energy surface are studied.

Computational Procedure

The cluster model is one of the most popular models used in theoretical studies of the solid state. A molecule is surrounded by other molecules, geometrically arranged in accordance with space group symmetry. When the overlap between the central molecule and its nearest neighbors is nonnegligible, one treats a cluster of molecules quantum mechanically (supermolecule or SM model). In this SM model, all $3N$ (for N atoms) degrees of freedom of the central molecule can be refined. These are the $3N - 6$ internal coordinates, the position of the center of mass, and the orientation of the inertial frame. The SM approach was successfully used for the geometry optimization of 2,3-diketopiperazine,[6] formamide oxime,[7] and three polymorphic forms (α, β, and γ) of glycine[8] in the solid state.

In this study, the structure and orientation of a CO_3^{2-} ion in a hydroxyapatite lattice were completely optimized using the ab initio Hartree−Fock MIA method[9] for the SCF calculations, a combination of the multiplicative integral approximation and the direct SCF method.[10] The standard gradient procedure of Pulay[11] was used for the evaluation of the forces on the atoms of the central CO_3^{2-} ion. In all calculations, a triple-ζ valence (TZV) basis set[12] was used, resulting in 584 contracted basis functions for the complete structure. The calculations were performed in parallel with the program BRABO[13] using the PVM software[14] on a cluster of IBM RS6000 workstations.

Information obtained from the experimental hexagonal crystal structure[15] was used to build a model for the apatite lattice, containing six Ca^{2+} ions and six PO_4^{3-} groups. This fragment of the crystal structure includes the local D_{3d} symmetry found in the crystal and was fixed during the calculations. A CO_3^{2-} ion is placed in the center of this cluster of Ca^{2+} and PO_4^{3-} ions. This represents calcium hydroxyapatite in which two OH^- groups, normally located in the channel along the $\bar{6}$ rotation axis in a head-to-tail fashion, are substituted by one CO_3^{2-} ion, resulting in A-type carbonated apatite.[1,16] The atom numbering for the central ion and the structure of the apatite cavity are shown in Figure 1. The symmetry axis (crystallographic *c* axis) is perpendicular to the plane of Figure 1.

To guarantee an unbiased starting model for the calculations, the carbonate ion was placed in the center of the cavity and was oriented in three different perpendicular planes. Two planes were parallel with the symmetry axis, and one was perpendicular to this *c* axis. The carbon atom was placed near the inversion center of the lattice. For the three different starting structures, the geometry of the crystal lattice was fixed and the carbonate ion was allowed to change its internal geometry, position, and orientation in the cavity during the optimization. The coordi-

[†] University of Antwerp; anik@uia.ua.ac.be, alsenoy@uia.ua.ac.be.
[‡] University of Ghent; erna.demaeyer@rug.ac.be, ronald.verbeeck@rug.ac.be.
[⊗] Abstract published in *Advance ACS Abstracts,* April 15, 1997.

S1089-5647(96)04041-2 CCC: $14.00

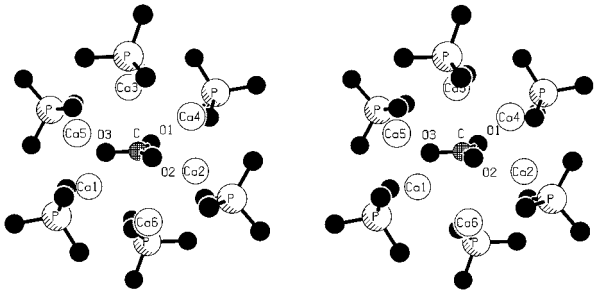

Figure 1. Stereoscopic illustration and atom numbering of the central A-type CO_3^{2-} impurity in the hydroxyapatite cavity with the *c* axis perpendicular to the plane of the figure.

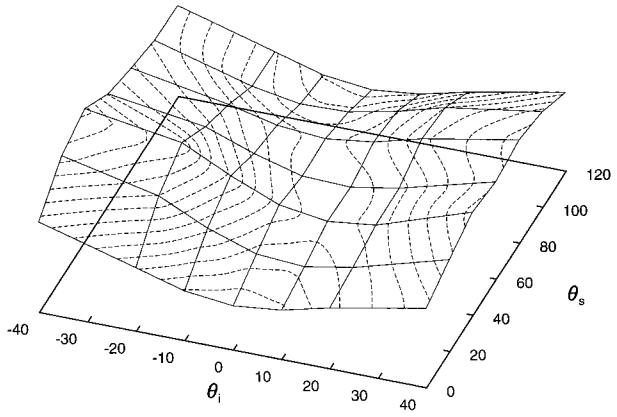

Figure 2. Potential energy surface for the rotation of CO_3^{2-} about the symmetry axis (θ_s) and the third axis of inertia (θ_i). Isoenergetic contour levels are shown on the grid.

nates proposed by Young et al.[4] were also used as a starting structure for an additional optimization. Structures were refined until all Cartesian force components were smaller than 0.001 mdyn. At this level of refinement, structural parameters are thought to be converged to 0.0002 Å for bond lengths and to 0.1° for angles.

In order to obtain information on the potential energy surface, a two-dimensional grid was defined by the rotation about the symmetry axis of the crystal lattice and the rotation about the third axis of inertia of CO_3^{2-}, which is oriented perpendicular to the plane of the molecule. For all points on the grid, single-point energy calculations were performed (Figure 2).

Results and Discussion

Geometry Optimization. The angle between the CO_3^{2-} plane and the symmetry axis was 7° after each optimization. This is in agreement with the findings of other authors, who report that the CO_3^{2-} plane is parallel with the symmetry axis[2,5] or makes an angle of less than 27° with it.[4,17] In Figure 1, a stereoscopic illustration of the optimized structure of CO_3^{2-} in the HAp cavity is given. The carbon atom is found along the symmetry axis, 0.1 Å below the inversion center. Two oxygen atoms also occupy positions close to this axis; one of these oxygen atoms (O1) is separated 0.7 Å from the center of the triangle formed by the three lower Ca^{2+} ions (Ca1, -2, and -3 in Figure 1), whereas the second oxygen atom (O2) is 0.8 Å away from the center of the upper Ca triangle (Ca4, -5, and -6 in Figure 1). The third oxygen atom (O3) is removed 1.2 Å from the *c* axis and is found 0.15 Å below the plane midway between the Ca triangles.

The calculated positions are different from the CO_3^{2-} coordinates of the tetrahedral structure proposed by Young et al.[4] These authors also place the carbon atom along the *c* axis but closer to the upper Ca triangle. One of the oxygen atoms in their model is taking the position the carbon atom occupies in our model. The two remaining oxygens are only 0.35 Å below the plane formed by the upper three Ca^{2+}, ions and each of them is positioned in a different plane bisecting the line between two upper Ca^{2+} ions. When the carbonate structure proposed by Young et al.[4] was used as a starting point for a geometry optimization in the HAp cavity, it lead to an optimized structure identical to one of our minima.

TABLE 1: Geometrical Parameters for the CO_3^{2-} Ion in the Gas Phase and in a Hydroxyapatite Cavity. Van der Waals Interactions with Ca^{2+} Ions of the Crystal Cavity

	gas phase	apatite cavity
bond lengths, Å		
C−O1	1.3080	1.3053
C−O2	1.3080	1.3071
C−O3	1.3080	1.1874
valence angles, deg		
O1−C−O2	120.0	135.2
O1−C−O3	120.0	110.5
O2−C−O3	120.0	114.2
out-of-plane angles, deg		
O1 out of O3,O2,C plane	0.0	−0.62
O2 out of O3,O1,C plane	0.0	0.60
van der Waals distances, Å		
O1···Ca2		2.068
O1···Ca3		2.308
O2···Ca4		2.139
O2···Ca6		2.348
O3···Ca1		2.247
O3···Ca5		2.282

The D_{3d} symmetry of the environment results in six energetically and geometrically equivalent positions for the carbonate ion in the hole. A rapid interchange between the different orientations might explain why there is no experimental evidence on the exact position of the carbonate impurity in calcium hydroxyapatite. The nature of this rotation will be studied in more detail below.

In Table 1, the geometry of the CO_3^{2-} ion in the gas phase and in the hydroxyapatite lattice and the closest contacts with Ca^{2+} ions are given. In the apatite cavity, the C−O1 and C−O2 bonds have approximately the same length as in the gas phase, whereas the C−O3 bond shows double-bond character, because it is repelled by a phosphate oxygen that is only 2 Å apart. This C−O3 bond is oriented almost perpendicular to the symmetry axis of the crystal, whereas the two other bonds are pointing up and down this axis, with O2 and O1 respectively 0.95 and 0.55 Å removed from the positions the OH^- oxygen atoms would occupy in the pure hydroxyapatite lattice. The O1−C−O2 valence angle is the largest valence angle, allowing the O1 and O2 atoms to move as close to the OH^- positions as possible. The O1−C−O3 angle is smaller than the O2−C−O3 angle, indicating that O3 is tilted toward O1, which is toward the lower part of the crystal lattice in this case. If the CO_3^{2-} ion would be inverted in order to obtain one of the symmetry-related orientations, O3 would be tilted toward the upper part of the lattice. The out-of-plane angles indicate that the CO_3^{2-} ion in the apatite cavity is nearly planar, in contrast to the tetrahedral structure proposed by Young et al.[4]

Vibrational Characteristics. For the position and the geometry of the carbonate ion, described in Table 1, a complete harmonic force field was calculated. The resulting force constants, calculated by numeric differentiation of the gradients, were translated into vibrational absorptions. The calculated wavenumbers were scaled[18] by 0.85, except for the out-of-plane vibration, where a scaling factor of 0.95 was applied. The calculated wavenumbers can be compared with gas-phase

TABLE 2: Calculated and Experimental[2,3,18,19,21,25] Wavenumbers ($\bar{\nu}_c$ (cm^{-1}) and $\bar{\nu}_e$ (cm^{-1}), respectively), Assignment ν, Calculated Integrated Intensities A (km/mol), and Potential Energy Distribution[33] for Vibrations of CO_3^{2-} in the Gas Phase and of A-type CO_3^{2-} in a Hydroxyapatite Lattice

$\bar{\nu}_c$	$\bar{\nu}_e$	ν	A	potential energy distribution[a]		
			Gas Phase			
597			0.14	α_1(63%)	$-\alpha_2$(21%)	
597			0.14	α_2(63%)	α_1(21%)	
879			6.45	γ(100%)		
881			0.00	r_1(33%)	r_2(33%)	r_3(33%)
1236			77.23	r_3(42%)	$-r_2$(38%)	α_1(16%)
1236			77.23	r_1(53%)	$-\alpha_2$(16%)	$-r_2$(15%)
			Hydroxyapatite Lattice			
541	670	ν_4	1.36	α_1(63%)	r_1(20%)	r_2(15%)
808	757	ν_4	4.10	α_2(94%)		
880	877−883	ν_2	29.55	γ(98%)		
1043		ν_1	25.74	r_2(43%)	r_1(33%)	$-\alpha_1$(18%)
1332	1450−1465	ν_3	83.79	r_1(44%)	$-r_2$(38%)	$-\alpha_2$(19%)
1720	1525−1550	ν_3	111.05	r_3(85%)	α_1(10%)	

[a] Definition of internal coordinates for A-type CO_3^{2-}: r_1, C−O1 stretch; r_2, C−O2 stretch; r_3, C−O3 stretch; α_1, bend 2(O1−C−O2) − (O1−C−O3) − (O2−C−O3); α_2, bend, (O1−C−O3) − (O2−C−O3); γ, O1 out of (O2,O3,C) plane.

absorptions (scaled in the same way) and with experimental results in Table 2. For each vibrational mode, the procentual contribution of the different internal coordinates (potential energy distribution) is given. For convenience, contributions smaller than 10% are omitted from the table.

The two largest calculated wavenumbers (1332 and 1720 cm^{-1}) can be assigned to the ν_3 stretching mode in experiments. Because the CO_3^{2-} ion has C_3 symmetry in the gas phase, this band is degenerate (1236 cm^{-1}), whereas the vibrational wavenumbers found in the apatite cavity correspond to experimental wavenumbers found for CO_3^{2-} with C_{2v} symmetry. The largest wavenumber (1720 cm^{-1}) can be assigned to the C═O3 stretch.

The next mode in the calculated gas-phase spectrum is not IR active because it is a symmetric stretch (881 cm^{-1}). Due to the interaction with the lattice, the constitution of this band (ν_1) changes in the solid state and the vibration should be visible at approximately 1040 cm^{-1}. However, in apatite, this band is masked by the ν_3 absorption band of PO_4^{3-}.[1]

The value of the out-of-plane vibration (880 cm^{-1}) is apparently unaffected by the apatite cavity, although the peak should be stronger in the solid state according to the calculations. This vibration can be identified with the ν_2 bending mode found in experiments. The calculated wavenumber is very well in line with the experimental values (Table 2). Also, the calculated relative intensity of this band with respect to the ν_3 bands is in agreement with the experimental results.[1,2,19,20]

The remaining wavenumbers for internal vibrations can be assigned to the ν_4 bending mode. The low integrated intensities are in agreement with the experimental finding that these absorption bands can hardly be detected.[2,21−23]

Variation of the Lattice Parameters. The unit cell parameters for calcium hydroxyapatite obtained by different research groups vary between 9.403 and 9.49 Å for the *a* axis and between 6.866 and 6.940 Å for the *c* axis.[1,24,25] Moreover, the lattice dimensions vary with the A-type carbonate content. This variation has been well documented in the literature.[20,26−29] The *a* dimension systematically increases and the *c* dimension decreases with increasing carbonate content. To study the influence of the lattice parameters on the geometry of the central ion, the CO_3^{2-} ion was placed in three apatite lattices with different dimensions. Apart from the parameters for pure HAp used for the foregoing calculations,[15] the parameters mentioned on the ASTM datafile of HAp[30] were used, as well as the dimensions of an A-type carbonated apatite containing 4.39% CO_3^{2-}.[31]

TABLE 3: Effect of Variations of the Cell Parameters on the Optimized Geometry of the CO_3^{2-} Ion, the Position of the Center of Mass, and the Orientation of the Inertial Frame

	pure HAp[29]	pure HAp[15]	HAp with 4.39% CO_3^{2-} [30]
a axis, Å	9.418	9.424	9.544
c axis, Å	6.884	6.879	6.859
center of mass, Å	0.076	0.076	0.073
	0.015	0.015	0.009
	3.335	3.333	3.327
Euler angles, deg	−127.0	−127.0	−126.7
	−83.2	−83.2	−82.9
	92.2	92.2	92.2
bond lengths, Å			
C−O1	1.3054	1.3053	1.3033
C−O2	1.3073	1.3071	1.3064
C−O3	1.1871	1.1874	1.1934
valence angles, deg			
O1−C−O2	135.3	135.2	133.8
O1−C−O3	110.5	110.5	111.4
O2−C−O3	114.2	114.2	114.8

In Table 3, the internal geometry of the CO_3^{2-} ion as well as the position of the center of mass and the orientation of the inertial frame are given for the three different unit cells. It can be seen that the shortening of the *c* axis results in smaller C−O1 and C−O2 bond lengths and a smaller O1−C−O2 angle. The C−O3 bond, on the other hand, elongates with the *a* axis with increasing carbonate content because the lattice becomes wider and the O3···PO_4^{3-} distance increases. Conversely, it can be suggested that the repulsion between O3 and PO_4^{3-} causes the *a* dimension to increase with increasing A-type CO_3^{2-} incorporation. As can be seen from Table 3, the orientation of CO_3^{2-} in the HAp cavity as reflected by the Euler angles and the position of the center of mass are hardly influenced by the change in cell parameters. The effect of a variation of the cell dimensions on the internal and external coordinates of the carbonate ion is thus negligible. It can therefore be expected that the vibration characteristics will not be significantly influenced by this change in lattice dimensions either.

Charges on the Atoms. After the optimization of the structure and orientation of CO_3^{2-} in the HAp cavity, the resulting wave function was used to calculate the Mulliken charges on the different atoms.[32] O1 and O2, occupying the OH^- positions, carry a higher negative charge (−1.00e and −0.99e, respectively) than O3 (−0.65e). Because the carbon atom has a positive charge of +0.69e, the total charge on the CO_3^{2-} group is −1.95e. On the PO_4^{3-} groups, the charge is −2.88e and for the Ca^{2+} ions +1.87e. The total charge of the system, consisting of one CO_3^{2-}, six Ca^{2+}, and six PO_4^{3-} ions, is −8e. The fact that the charges on the ions are different from the charges of the isolated residues indicates that indeed the wave function in the SM model allows for overlap and charge transfer between the different charged groups in the system.

Study of the Potential Energy Surface. For the optimized structure (Table 1), the potential energy surface was studied in order to obtain a reasonable estimate for the path between structures related by the 3-fold axis. For the conversion between two symmetry-related structures, two possible mechanisms had to be considered. The most probable reaction path is the 120° rotation about the crystallographic *c* axis. In that case, the

internal geometry of the CO_3^{2-} ion is unaffected. However, it is also possible that the molecule performs an in-plane rotation in combination with a 60° rotation about the symmetry axis, thereby elongating the C═O3 bond and shortening one of the other C—O bonds.

Therefore, one axis of the two-dimensional grid describes the rotation about the symmetry axis of the crystal lattice. The angle varies between 0° and 120° with a step size of 20°. As a second degree of freedom, the rotation about the third axis of inertia of CO_3^{2-} was chosen, which is oriented perpendicular to the plane of the molecule. For this second axis, rotations of −40°, −20°, −10°, 0°, 10°, 20°, and 40° were chosen. For all 49 points on the grid, single-point energy calculations were performed. The resulting isoenergetic contour levels are shown in Figure 2.

Due to the higher energy barrier for rotation about the inertia axis, the second mechanism can be rejected. When the CO_3^{2-} ion is rotated about the symmetry axis as proposed in the first mechanism, close contacts with Ca^{2+} ions and phosphate groups are avoided by small additional rotations about the inertia axis. An important advantage of this reaction path is the possibility of passing through an intermediate minimum after rotating 60°. The intermediate structure with the C—O3 bond pointing in the upward direction is energetically equivalent to the starting structure but is not shown in Figure 2 because no geometry optimizations were performed for the points on the grid. All points refer to the structure as given in Table 1.

Conclusions

With the aid of quantum chemical ab initio calculations using the supermolecule model, it has been possible to study the geometry, position, and orientation of an A-type CO_3^{2-} impurity in a hydroxyapatite lattice. The calculated angle between the planar CO_3^{2-} ion and the *c* axis is 7°. The carbon atom and two oxygen atoms are found close to this axis, whereas the bond with the third oxygen atom is almost perpendicular to it. The latter bond is a C═O double bond, whereas the two other C—O bonds are single bonds.

The calculated wavenumbers of the vibrational absorptions are in reasonable agreement with the experimentally available values.

The effect of experimentally observed variations of the unit cell parameters on the internal and external geometries of the CO_3^{2-} impurity is negligible.

A study of the potential energy surface indicated that two minimal energy positions are related by rotation about the crystallographic *c* axis.

Acknowledgment. C.V.A., A.P., and E.D.M. thank the Belgian National Fund for Scientific Research for an appointment as Research Director (C.V.A.) or Senior Research Assistant (A.P. and E.D.M.).

References and Notes

(1) Driessens, F. C. M.; Verbeeck, R. M. H. *Biominerals*; CRC: Boca Raton, FL, 1990.
(2) Elliott, J. C. The interpretation of the infra-red absorption spectra of some carbonate-containing apatites. In *Tooth enamel*; Stack, M. V., Fearnhead, R. W., Eds.; John Wright: Bristol, 1965; p 20.
(3) Elliott, J. C.; Holcomb, D. W.; Young, R. A. *Calcif. Tissue Int.* **1985**, *37*, 372.
(4) Young, R. A.; Bartlett, M. L.; Spooner, S.; Mackie, P. E. *J. Biol. Phys.* **1981**, *9*, 1.
(5) Doi, Y.; Aoba, T.; Moriwaki, Y.; Okazaki, M.; Takahashi, J. *J. Dent. Res.* **1980**, *59* (9), 1473.
(6) Peeters, A.; Van Alsenoy, C.; Lenstra, A. T. H.; Geise, H. J. *Int. J. Quantum Chem.* **1993**, *46*, 73.
(7) Peeters, A.; Van Alsenoy, C.; Lenstra, A. T. H.; Geise, H. J. *THEOCHEM* **1994**, *304*, 101.
(8) Peeters, A.; Van Alsenoy, C.; Lenstra, A. T. H.; Geise, H. J. *J. Chem. Phys.* **1995**, *103*, 6608.
(9) Van Alsenoy, C. *J. Comp. Chem.* **1988**, *9*, 620.
(10) Almlöf, J.; Faegri, K.; Korsell, K. *J. Comp. Chem.* **1982**, *3*, 385.
(11) Pulay, P. *Mol. Phys.* **1969**, *17*, 197. Pulay, P. *Theor. Chim. Acta* **1979**, *50*, 299.
(12) Schäfer, A.; Huber, C.; Ahlrichs, R. *J. Chem. Phys.* **1994**, *100*, 5829.
(13) Van Alsenoy, C.; Peeters, A. *THEOCHEM* **1993**, *286*, 19.
(14) Geist, A.; Beguelin, A.; Dongarra, J.; Jiang, W.; Manchek, R.; Suderam, V. PVM: Parallel Virtual Machine. *A Users' Guide and Tutorial for Networked Parallel Computing*; MIT: Cambridge, MA, London, 1994.
(15) Sudarsanan, K.; Young, R. A. *Acta Crystallogr.* **1969**, *B25*, 1534.
(16) De Maeyer, E. A. P.; Verbeeck, R. M. H. *Bull. Soc. Chim. Belg.* **1993**, *102* (9), 601.
(17) Elliott, J. C. *Calc. Tiss. Res.* **1969**, *3*, 293.
(18) Pulay, P. *Modern electronic structure theory, Part II*; Yarkony, D. R., Ed.; World Scientific: Singapore, 1995; p 1191. Hehre, W. J.; Radom, L.; Schleyer, P. v. R.; Pople, J. A. *Ab initio molecular orbital theory*; Wiley: New York, 1986; p 226.
(19) Montel, G. *Bull. Soc. Chim. Fr.* **1968**, 1694.
(20) Bonel, G. *Ann. Chim.* **1972**, *7*, 65.
(21) Nelson, D. G. A.; Featherstone, J. D. B. *Calcif. Tissue Int.* **1982**, *34*, S69.
(22) El Feki, H.; Rey, C.; Vignoles, M. *Calcif. Tissue Int.* **1991**, *49*, 269.
(23) De Maeyer, E. A. P. Ph.D. Thesis, University of Ghent, Ghent, Belgium, 1992.
(24) Wallaeys, R. *Ann. Chim.* **1952**, *7*, 808.
(25) Carlström, D. *Acta Radiol.* **1955**, supplem. 121.
(26) LeGeros, R. Z.; Trautz, O. R.; Klein, E.; LeGeros, J. P. *Sep. Exp.* **1969**, *24*, 5.
(27) LeGeros, R. Z.; LeGeros, J. P.; Trautz, O. R.; Klein, E. *Dev. Appl. Spectrosc.* **1970**, *7B*, 3.
(28) Young, R. A. *Clin. Orthop.* **1975**, *113*, 249.
(29) Elliott, J. C.; Bonel, G.; Trombe, J. C. *J. Appl. Crystallogr.* **1980**, *13*, 618.
(30) ASTM Powder Diffraction File No. 9-432.
(31) Elliott, J. C. *J. Dent. Res.* **1963**, *42*, 1081.
(32) Mulliken, R. S. *J. Chem. Phys.* **1955**, *23*, 1833.
(33) Califano, S. *Vibrational States*; Wiley: London, 1976; p 235.